A COMPARATIVE STUDY OF HIGH INTERNAL PHASE EMULSIONS (HIPEs) STABILIZED WITH PROTEINS FROM MEALWORM (*Tenebrio molitor*) AND BLACK SOLDIER FLY (*Hermetia illucens*)

Chiara Rusciano

Departament d'Enginyeria Química. Universitat Rovira i Virgili,
EscolaTècnica Superior Enginyeria Química, Avinguda Països Catalans 26,
Campus Sescelades, 43007 Tarragona, Spain.

ABSTRACT

To address the demand for plant oil-based analogues of adipose tissue as sustainable alternatives to animal fat, high internal phase emulsions (HIPEs) were developed using insect-derived proteins as stabilizers and compared with HIPEs stabilized by whey protein. This study aims to evaluate the potential of insect proteins in forming 3D-printable emulsions that mimic the structural and functional properties of animal fat. HIPEs with an oil phase of 75% were successfully formulated, exhibiting a droplet size distribution ranging from 23 to 33 μm. Emulsion stability was monitored over a 22-day storage period. The emulsion stabilized with 4% WPI remained stable throughout the entire period, whereas those stabilized with insect proteins maintained stability for less than 7 days, with the exception of the one containing 2.5% BSF, which remained stable up to day 7. The results indicated that emulsions stabilized with insect proteins possessed rheological characteristics more suitable for 3D printing than those based on whey protein (i.e., higher viscosity and improved viscoelastic behavior). Although the emulsions maintained structural stability for an average of 7 days, insect-derived proteins showed promising potential as functional and sustainable emulsifiers in the formulation of fat analogues.

1 Introduction

Among the various types of emulsions, high internal phase emulsions (HIPEs) have attracted increasing interest due to their structural and rheological properties. An HIPE is an emulsion where the internal phase volume fraction exceeds the close packing limit (typically >74%), which leads to tightly packed droplets that, in most cases, adopt polygonal shapes (Fuhrmann et al., 2022). As a result of the close packing of the droplets, these emulsions are no longer in a liquid state, but they can exhibit both elastic and viscous properties due to their soft solid structure.

Due to their unique properties, HIPEs have gained relevance in a wide range of applications, including cosmetics, pharmaceuticals, and food products (Gao et al., 2021). In the food industry, HIPEs are being investigated for their potential to develop healthier formulations rich in unsaturated fatty acids and to replicate the texture of adipose tissue. Their 3D printability enables the design of microstructures that closely mimic real fat tissue. This feature offers a promising strategy to enhance the resemblance of plant-based products to their animal-based counterparts, aligning with the growing demand for plant-based meat alternatives driven by environmental, ethical, and health considerations (Hu & McClements, 2022).

Traditionally, small-molecule synthetic surfactants have been widely used to stabilize HIPEs. Common examples include cetyl trimethylammonium bromide (CTAB), Tween 20, and Tween 80. Recently, however, there has been growing interest in the use of natural emulsifiers, owing to their favorable functional properties and increasing consumer concern regarding animal-derived and synthetic ingredients in food products. In this context, biopolymer-based surfactants have received significant attention, particularly polysaccharides and proteins.

Proteins are natural polymers composed of amino acids that vary in type, sequence, and number. Consequently, they exhibit diverse functional and nutritional effects in food systems. Proteins are widely used as functional ingredients in oil-in-water (O/W) emulsions due to their excellent

emulsifying properties. They stabilize emulsions by forming a viscoelastic adsorbed layer at the oil–water interface, preventing coalescence through steric hindrance and electrostatic repulsion. This is made possible by the presence of both hydrophilic and hydrophobic amino acid residues within the protein structure (Zhang et al., 2022). Proteins can be derived from either plant or animal sources, which not only affects their functional characteristics but also influences consumer acceptance. Common animal-derived proteins used in HIPEs stabilization include whey protein (milk) (G. Liu, Li, Qin, & Zhong, 2020), casein (milk) (Yan et al. 2024), gelatin (meat or fish) (Du et al. 2024), and ovalbumin (egg) (Hyust et al. 2023). Recently, there has been increasing interest in plant-based alternatives due to sustainability and ethical concerns. Typical plant-derived proteins used in HIPEs include gliadin (Huang et al. 2019), soy protein (Sun et al. 2024), peanut protein (Shi et al. 2020), and zein (Wang et al. 2025). These are favored for their good emulsifying capacity, high availability, and relatively low cost.

Insect proteins have emerged as a sustainable alternative to conventional protein sources. Compared to traditional livestock farming, insect farming generates fewer greenhouse gas emissions and requires significantly less water (van Huis et al., 2013). Moreover, proteins extracted from various insect species have demonstrated emulsifying capacities comparable to those of dairy proteins and superior to many plant-based proteins in stabilizing O/W emulsions (Wang et al., 2021).

Several studies have investigated alternative insect protein sources for the stabilization of O/W emulsions (Table 1). Bußler et al. (2016) highlighted the functional properties of proteins extracted from *Tenebrio molitor* (TM) and *Hermetia illucens* (BSF), emphasizing their potential as sustainable and effective emulsifying agents. Notably, Gould and Wolf (2018) demonstrated that O/W emulsions stabilized with TM proteins exhibited no significant changes in droplet size even after two months of storage at room temperature. Ballon et al. (2025) recently explored the potential of insect proteins in stabilizing HIPEs intended for use as 3D printable fat analogues. Jiang et al. (2023) examined the use of ultrasonic treatment to stabilize high internal phase emulsions (HIPEs) using silkworm pupa

protein (SPP) as the sole emulsifier Nevertheless, whey protein isolate (WPI) remains the industry benchmark, owing to its superior solubility and rapid interfacial adsorption kinetics (Foegeding & Davis, 2011).

The specific objective of this master's thesis was to assess the potential of two different insect proteins, extracted from TM and BSF powder, to develop printable HIPEs suitable for formulating fat analogues. The performance of TM and BSF proteins to stabilize HIPEs was compared to that of whey protein isolate (WPI), a dairy protein commonly used as emulsifier in food applications. To do so, O/W HIPEs (75 wt% sunflower oil) were formulated using TM and BSF proteins, as well as WPI. Their physical stability was assessed during storage at room temperature, and rheological properties were analyzed. Finally, the printability of the HIPEs was evaluated.

Table 1 Examples of application of insect proteins as emulsifiers.

Insect species	Oil fraction and emulsion type	Protein concentration	Emulsification technology	Main results	Reference
Alphitobius diaperinus *Acheta domesticus*	O/W HIPEs 80% (w/w) sunflower oil	0.5-3%	High-speed homogenizer	HIPEs stable for 14 days at room temperature were obtained, suitable to be used as ink for 3D printing.	Ballon et al. (2025)
Alphitobius diaperinus	$W_1/O/W_2$ double emulsion, 14% (w/w) sunflower oil	1%	High-speed homogenizer and dynamic membranes of tunable pore size	Good stability under simulated digestion and processing; suitable for bioactive delivery; droplet size distribution and stability at 4°C comparable to the emulsions produced with WP.	Wang, Ballon et al. (2021)
Bombyx mori	O/W HIPE, 78% (w/w) soybean oil	2.0%	High-speed homogenizer	Stable intestine-targeted Pickering emulsions with high encapsulation efficiency	Jiang et al. (2023)
Hermetia illucens	O/W 20-40% (w/w) sunflower and lemon oil	1%, 2%	High-speed homogenizer and dynamic membranes of tunable pore size	High emulsion stability; potential for sustainable food formulation	Wang, Jousse et al. (2021)
Tenebrio molitor	O/W, 10% (v/v) corn oil	1.0–3.0%	High-speed homogenizer	Stable emulsions with freeze-thaw and heat treatments.	Gkinali et al. (2023)
Tenebrio molitor	O/W emulsions, 20% (w/w) sunflower oil	0.44%, 0.88%, 1.75%, 2.63%	High shear overhead mixer	Stable O/W emulsions without significant droplet coalescence for a period of at least 2 months; lower droplet size when compared to WP; resistance to coalescence for frozen and heating up to 80°C	Gould and Wolf (2018)
Tenebrio molitor	O/W HIPEs 50-80% (v/v) corn oil	0.5-2.5%	High-speed homogenizer	Good emulsifying properties of TM for HIPEs and drug delivery systems.	Huang et al. (2022)

2 Materials and methods

2.1 Materials

Proteins used include proteins extracted from edible mealworm (*Tenebrio molitor*) powder (Tebrio Transformacion SL - España), edible black soldier fly (*Hermetia illucens*) powder (Brown Foods Biotech- España) and whey protein isolate (WPI) (98.0% purity, Davisco Foods International, Le Sueur, MN, USA). The soluble protein content in solution was quantified using a Pierce™ BCA protein assay kit (ThermoFisher Scientific, Waltham, MA, USA). The concentrations were expressed in bovine serum albumin equivalent (BSAE%, w/w) and are shown in % for simplicity. Sunflower oil was bought from a local supermarket. Deionized water was used for the preparation of the samples.

2.2 Defatting of insect powders and protein extraction

Defatting of the insect powders was conducted by mixing 100 g of powder with 500 ml of hexane at 500 rpm for 1.5 h. The mixtures were then left to stand for 20 min in order to reach the phase separation. The solvent phase containing the lipids was decanted and the remaining solid phase was stirred again with 500 ml of hexane at 700 rpm for 1 h. After decantation, the residual powder was kept under the fume hood for 24 hours in order to have complete evaporation of hexane. The solvent was recovered using the rotary evaporator and reused.

Tenebrio molitor protein concentrate (TMPC) and black soldier fly protein concentrate (BSFPC) were obtained by alkaline solubilization followed by acid precipitation at their isoelectric point, following a slightly modified version of the method developed by Wang, Ballon et al. (2021) research group. In brief, 30 g of defatted insect powder was mixed with 300 mL of 0.25 M NaOH and stirred for 1 h at 40 °C. Then, the sample was centrifuged for 15 min at 4490 rpm to obtain 2 phases. The supernatant was collected, and the procedure was repeated once on the remaining pellet. The combined supernatants from the 2 extractions were adjusted to pH 3-4 using 35% of HCl, followed by

centrifugation at 3790 rpm for 15 min. The precipitated proteins were freeze-dried (LYOQUEST-85 PLUS, Telstar, Barcelona, Spain) for 36 h, ground, and stored in plastic bags in desiccator at 4 °C. The protein content of the protein concentrate obtained was not determined during this project.

2.3 Preparation of the HIPEs

The WPI solution was prepared by stirring 5 g of WPI and 50 g of deionized water for 2 h. The solution was stored overnight at 4 °C.

TMPC and BSFPC solutions were prepared by dispersing 5 g of protein concentrate in 50 g of deionized water, followed by continuous stirring for 2 h. The pH of the mixture was adjusted to 7 after 30 min, 1 h, and 2 h of stirring by adding 4M NaOH. Solutions were stored overnight at 4 °C. The following day, the TMPC and BSFPC protein suspensions were centrifuged (10 min, 4500 rpm) to remove insoluble proteins. The supernatant was collected, and its protein concentration was determined using the BCA assay kit. Sodium azide (0.02%) was added to the supernatant to prevent microbial growth.

HIPEs were produced by mixing sunflower oil (75 wt%) with the protein solution (25 wt%) containing either 2.5% or 4% protein, in a 50 mL plastic tube. The oil was gradually added to the protein solution during homogenization at 15000 rpm (Ultra Turrax T18 digital, IKA, Staufen, Germany) for approximately 8 minutes. All the emulsions were prepared in duplicates.

2.4 Physical stability of the HIPEs

The emulsions were stored in the 50 ml plastic tube for 21-22 days at room temperature (25 ± 2 °C) and their physical stability was studied during storage by following the changes in visual appearance, droplet size, ζ-potential, and oil loss after 1, 2 and 3 weeks.

2.4.1 Microstructure

The microstructure of the HIPEs was analyzed at room temperature using a microscope (Primovert, Carl Zeiss AG, Oberkochen, Germany), equipped with a camera (SpeedCam MacroVis EoSens, High Speed Vision GmbH, Ettlingen, Germany) under 20x and 40x objective.

2.4.2 Droplet size distribution and ζ-potential

The droplet size distribution was analyzed by laser diffraction using a Mastersizer 2000 (Malvern Instruments, Worcestershire, UK) with a refractive index set to 1.472 and 1.330 for sunflower oil and water, respectively. The emulsions were diluted around 10 times using deionized water. The mean droplet size and droplet size distribution width was reported as volume-weighted mean diameter ($d_{4,3}$) and span, calculated according to Equation (1) and Equation (2), respectively.

$$d_{4,3} = \frac{\sum n_i \cdot {d_i}^4}{\sum n_i \cdot {d_i}^3} \quad (1)$$

Where d_i is the droplet diameter of the ith size class and n_i is the number of droplets of diameter d_i.

$$span = \frac{d_{90} - d_{10}}{d_{50}} \quad (2)$$

Where d_x is the droplet diameter corresponding to x% volume on the cumulative droplet size distribution curve.

The surface charge of the emulsion droplets was measured by electrophoretic light scattering using a Zetasizer Nano ZS (Malvern Instruments, Worcestershire, UK) at 25 °C. Emulsions were diluted in deionized water. The ζ-potential was calculated using the Smoluchowski model.

The measurements of droplet size distribution and ζ-potential were performed in triplicate for each emulsion.

2.4.3 Oil loss

The oil loss was determined was determined according to Galvão et al. (2022) slightly modified, by placing around 1 g of emulsion in an Eppendorf tube (previously weighed) followed by centrifugation at 9000 rpm for 30 min. After centrifugation, the Eppendorf tubes were placed upside down for 2 h to remove the free oil. The Eppendorf tubes without oil were then weighed and the oil loss (OL) was calculated according to Equation (3):

$$OL(\%) = \frac{m_i - m_f}{m_i - m} \quad (3)$$

Where m_i is the initial weight of the Eppendorf tube with the sample, m_f is the weight of the Eppendorf tube with the sample after removing the free oil, and m is the weight of the empty Eppendorf tube. All the measurements were done in duplicates for each repetition.

2.5 Rheological characteristics

The rheological properties of the HIPEs were characterized at 25 °C in terms of flow behavior and viscoelastic properties using a Discovery HR20 rheometer (TA instruments, New Castle, DE, USA) with a parallel plate geometry (40 mm, 1 mm gap). The rheometer was equipped with a Peltier system for temperature control. The emulsions were pre-sheared at 0.01 s^{-1} for 1 min prior to the measurement. All the measurements were performed in duplicate. Amplitude sweeps were conducted using a strain ranging from 0.01 to 100%, at a fixed frequency of 10 rad/s, to determine the linear viscoelastic region (LVR). The storage (or elastic) modulus (G′) and the loss (or viscous) modulus (G″), as well as the oscillation stress were measured. Frequency sweeps were performed from 1 to 600 rad/s at a fixed strain of 0.1 %, within the LVR identified. The flow behavior was assessed by measuring the apparent viscosity over a shear rate range of 0.001 to 100 s^{-1}.

2.6 3D Printing

The HIPES were printed at room temperature (25 °C) using a commercial, extrusion-based, food grade 3D printer (Foodini, Natural Machines Iberia S.L., Barcelona, Spain) equipped with a 1.5 mm diameter nozzle. Printing parameters were selected based on Ballon et al. (2025) and included a printing speed of 850 mm/min, an ingredient flow speed of 2 (dimensionless), a line thickness of 1.4 mm, and a distance between layers of 1.6 mm. The insect protein-stabilized HIPEs were printed in the shape of a 3 layers hollow cylinder, while the WPI-stabilized HIPEs were printed in a heart shape. Printed figures were stored at room temperature for 7 days.

2.7 Statistical analysis

Data are presented as mean ± standard deviation. Statistical significance was assessed using one-way analysis of variance (ANOVA), with a significance threshold set at $p < 0.05$. All analyses were performed using OriginPro statistical software.

3 Results and discussion

3.1 Production of the HIPEs and visual appearance

HIPEs comprising 75 wt% sunflower oil were successfully prepared using aqueous phases containing TMPC and BSF at concentrations of 2.5% and 4% and compared with 4% WPI-stabilized emulsions.

All the emulsions exhibited good shape stability. Emulsions stabilized with 4% TM and 2.5% BSF proteins exhibited greater firmness and stability compared to those containing 2.5% TM and 4% BSF.. The WPI-stabilized HIPEs presented a creamier morphology respected to the insect-formulated, which tended to be more compact (Fig.1)

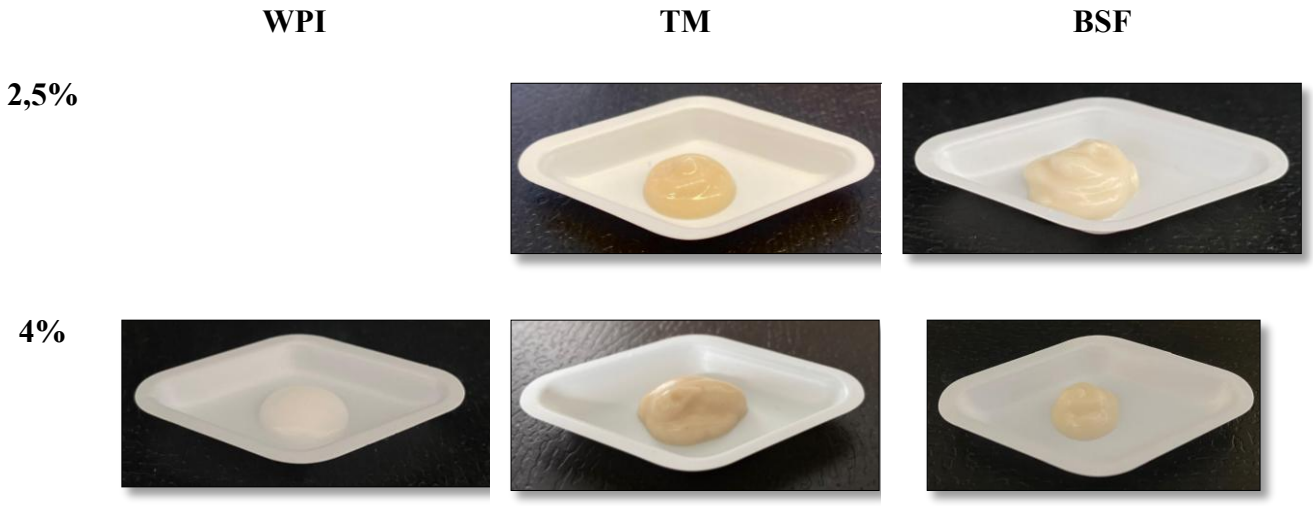

Figure 1 Visual appearance of the HIPEs stabilized with WPI, TM and BSF.

3.2 Physical stability

Physical stability of the HIPEs was determined during storage at room temperature for 0, 14, and 21 or 22 days. To do so, we monitored the progress of droplet size distribution, ζ-potential, oil loss and emulsion microstructure. After 7 days of storage, emulsions stabilized with 2.5%, 4% TM and 4% BSF exhibited clear phase separation and were consequently excluded from further characterization. The emulsion stabilized with 2.5% BSF remained stable until day 14, after which it also showed separation and was subsequently only analyzed for oil loss.

3.2.1 Droplet size and microstructure

The results of the particle size distribution analysis revealed that the emulsion stabilized with 4% WPI exhibited a unimodal profile, with a single population of droplets ranging between 10 and 100 µm. In contrast, emulsions stabilized with insect-derived proteins (BSF and TM) displayed a bimodal distribution, characterized by a secondary peak in the lower size range (0.8–8 µm).

Quantitative analysis was carried out using the volume-weighted mean diameter ($d_{4,3}$) and the span index, which provide insight into average droplet size and the breadth of the size distribution, respectively. HIPEs stabilized with 4% WPI exhibited an initial $d_{4,3}$ of approximately 31 μm, whereas those stabilized with insect proteins showed $d_{4,3}$ values ranging between 23 and 33 μm. For both TM and BSF proteins, increasing the protein concentration in the aqueous phase from 2.5% to 4% resulted in smaller droplet sizes. The 4% WPI-stabilized formulation demonstrated excellent temporal stability, with no significant changes in $d_{4,3}$ and span observed over a 22-day storage period. In contrast, HIPEs stabilized with insect proteins showed reduced stability during storage. Notably, the emulsion stabilized with 2.5% BSF protein displayed a progressive increase in $d_{4,3}$ over 7 days, indicative of droplet coalescence and a gradual decline in structural integrity (Figure 1).

Microscopy observations supported the particle size data. Due to the high internal phase ratio, the droplets were not perfectly spherical but instead adopted polygonal—mostly hexagonal—shapes, particularly evident in the WPI-based emulsions. This is indicative of a high packing efficiency and structural uniformity, which remained consistent over time. In contrast, emulsions stabilized with BSF and TM proteins exhibited a more irregular and heterogeneous microstructure, with a greater size variability (Figure 1). These findings are in agreement with the broader and bimodal size distributions observed via laser diffraction analysis, and they highlight the critical role of the emulsifying agent in governing both the initial architecture and long-term stability of HIPE systems.

These results are consistent with those reported for other insect protein-stabilized HIPEs, such as those by Ballon et al. (2023). Similarly, Jiang et al. (2023) observed $d_{4,3}$values ranging from 70 to 100 μm in HIPEs containing 78% (w/w) soybean oil stabilized with 2% silkworm pupae protein. Huang et al. (2022) reported a broader droplet size distribution, with diameters between 20 and 300 μm, in emulsions prepared with 80% (v/v) corn oil and TM proteins.

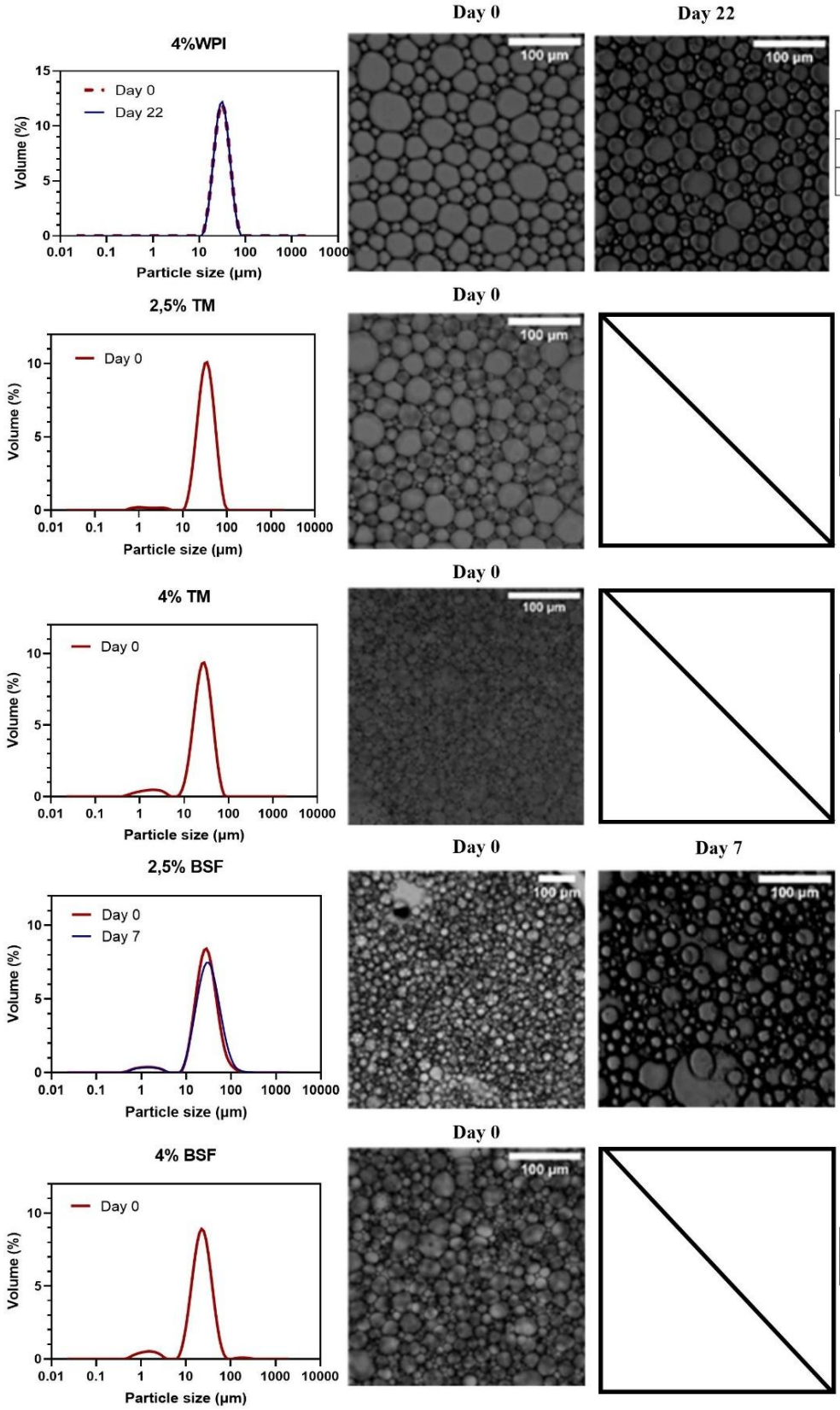

	Span	d[4,3]
Day 0	0,965±0,028	30,66±0,37 ^{A}
Day 22	0,954±0,030	30,72±0,39 ^{A}

	Span	d[4,3]
Day 0	1,172±0,050	33,25±1,14

	Span	d[4,3]
Day 0	1,308±0,023	25,53±0,53

	Span	d[4,3]
Day 0	1,524±0,266	29,22±4,09 ^{A}
Day 7	1,734±0,124	33,22±3,01 ^{B}

	Span	d[4,3]
Day 0	1,393±0,072	23,29±1,32

Figure 2 Droplet size distribution and microstructure of the HIPEs stabilized by WPI, TM and BSF. Capital letters indicate significant differences ($p < 0,05$).

3.2.2 ζ-potential

The ζ-potential is a measure of the surface charge of the droplets. When its absolute value exceeds ±30 mV, electrostatic repulsion between droplets is considered sufficient to ensure stability. All the HIPEs presented, from day 0, an adequate value of ζ-potential (ranging from -36,4 to -49,3 mV) (Table 1). The 4% WPI emulsion exhibited a statistically significant change in ζ-potential from day 0 to day 22, characterized by an increase in the absolute value. On day 0, the 2.5% TM, 2.5% BSF, and 4% BSF emulsions showed no significant differences among each other, whereas both the 4% WPI and 4% TM samples differed significantly from these and also from each other.

Table 2 ζ-potential of the HIPEs stabilized with WPI, TM and BSF at day 0, day 7, day 14 and day 22.

		ζ-potential (mV)			
		Day 0	**Day 7**	**Day 14**	**Day 22**
WPI	**4%**	-36,4±4,7 $^{A, a}$	-41,3±3,5 ^{B}	-44,5±2,7 ^{B}	-43,6±4,0 ^{B}
TM	**2,5%**	-41,4±1,6 ^{b}	Phase separation	Phase separation	Phase separation
	4%	-49,3±2,9 ^{c}	Phase separation	Phase separation	Phase separation
BSF	**2,5%**	-43,7±2,1 $^{A, b}$	-32,2±3,4 ^{B}	Phase separation	Phase separation
	4%	-42,9±2,5 ^{b}	Phase separation	Phase separation	Phase separation

Capital letters indicate significant differences within the same sample over different days, while lowercase letters indicate significant differences between different samples on day 0 ($p<0,05$).

3.2.3 Oil loss

Table 3 presents the oil loss percentages over a 22 day storage period. The 4% WPI HIPE exhibits a progressive increase in oil loss, starting from approximately 1.5% and rising to around 7% by day 14, after which it stabilizes. This trend suggests a potential destabilization of the emulsion structure occurring around day 14. However, the stabilization observed between day 14 and 21 may indicate the formation of a more stable separated phase. Although no major structural changes in the emulsion

are observed between day 0 and day 22, oil loss continues to rise over time. This trend is consistent with previous findings in the literature, where oil loss of WPI-stabilized emulsions reached approximately 8% by day 14 (Ballon et al., 2025). Similarly, Galvão et al. (2022) analyzed lentil protein isolate and reported a constant droplet size distribution over time, while oil loss progressively increased, reaching 8% by day 20.

Due to phase separation, it was possible to determine the oil loss at day 7 only for the 4% BSF emulsion, that was consistent with the minimal change in particle size distribution over time. However, the accuracy of the oil loss measurement method appeared to be limited. This may be attributed to an uneven distribution of the sample within the Eppendorf tubes. In some cases, the samples were completely expelled upon inversion, while in others, phase separation was evident in the sample but not reflected in the tube, likely due to inhomogeneous filling.

Table 3 Oil loss [%] of the HIPEs stabilized with WPI, TM and BSF at day 0, day 7, day 14 and day 22.

		Oil loss [%]			
		Day 0	**Day 7**	**Day 14**	**Day 22**
WPI	**4%**	1,1±0,5	1,7±0,1	7,1±0,9	7±0,4
TM	**2,5%**	1,6±0,5	Phase separation	Phase separation	Phase separation
	4%	0,9±0,2	Phase separation	Phase separation	Phase separation
BSF	**2,5%**	0,7±0,5	0,4±0,4	Phase separation	Phase separation
	4%	0,7±0,4	Phase separation	Phase separation	Phase separation

3.3 Rheology

Rheological characterization of the HIPEs was conducted through flow sweep, amplitude sweep, and frequency sweep tests. The flow sweep was performed to assess the viscosity and identify the presence of shear-thinning behavior. The frequency sweep was used to evaluate the storage modulus

(G′) and loss modulus (G″) as functions of frequency, while the amplitude sweep was carried out to determine the *Linear Viscoelastic Region* (LVR).

The flow sweep results confirmed a shear-thinning behavior (Figure 3), indicating that possible droplet aggregates are disrupted and that the droplets progressively align in the direction of the flow under increasing shear stress under increasing shear stress, as evidenced by the decrease in viscosity with increasing shear rate. At a shear rate of 10^{-3} s^{-1}, the viscosity of the WPI emulsion was approximately 2275 Pa·s, whereas the emulsions stabilized with 2.5% TM and 4% TM showed markedly higher values of 17193 Pa·s and 25212 Pa·s, respectively. Similarly, the emulsions with 2.5% BSF and 4% BSF reached viscosities of 8436 Pa·s and 14128 Pa·s. Furthermore, increasing the protein concentration led to a substantial rise in viscosity, indicating the formation of a more structured and resistant matrix at higher concentrations. However, it is worth noting that the slope of the G′ versus frequency curve remained close to −1 across all samples and may suggest the presence of wall slip. Given the high oil content of the emulsions, a parallel plate geometry was used for the measurements and this configuration, however, may have amplified wall slip effects. To reduce such artifacts, the use of sandblasted (roughened) plates might have provided more accurate rheological data by enhancing adhesion between the sample and the geometry surfaces.

The frequency sweep (Figure 4) revealed a typical gel-like response, with G′ consistently higher than G″ across the entire frequency range, highlighting the dominant elastic nature of the emulsions. For instance, at 10 rad/s, the G′ of the 4% TM emulsion was approximately 2400 Pa, compared to 850 Pa for the 2.5% TM emulsion. The 4% BSF emulsion reached G′ values of 1550 Pa, while WPI (4%) displayed the lowest modulus, around 400 Pa. These results indicate that TM-stabilized emulsions form a stronger and more cohesive gel network compared to both WPI and BSF, especially at higher protein concentrations.

In the amplitude sweep (Figure 5), all samples exhibited a linear viscoelastic region (LVR) at low strain, where G′ remained constant and higher than G″. Upon exceeding a critical strain threshold,

both moduli decreased, indicating the onset of structural breakdown and non-linear viscoelastic behavior. The crossover point (where G′ = G″) occurred at similar strain values for both 2.5% and 4% TM-stabilized emulsions, around 20%, suggesting that increasing TM concentration enhances the elastic modulus within the LVR but does not significantly affect the strain resistance at which structural breakdown begins. In contrast, BSF-stabilized emulsions showed a shift in the crossover point with concentration: approximately 10% for 2.5% BSF and 15% for 4% BSF, indicating improved mechanical stability at higher protein content. The 4% WPI emulsion displayed the lowest strain tolerance, with a crossover point at around 9%. Additionally, 4% BSF emulsions exhibited the highest initial G′ within the LVR (e.g., G′ ≈ 2300 Pa at 0.005 strain), along with the widest linear region, reflecting superior emulsion strength and elasticity. Overall, these results confirm that higher insect protein concentrations, particularly in BSF emulsions, enhance the structural integrity and viscoelastic robustness of the emulsions.

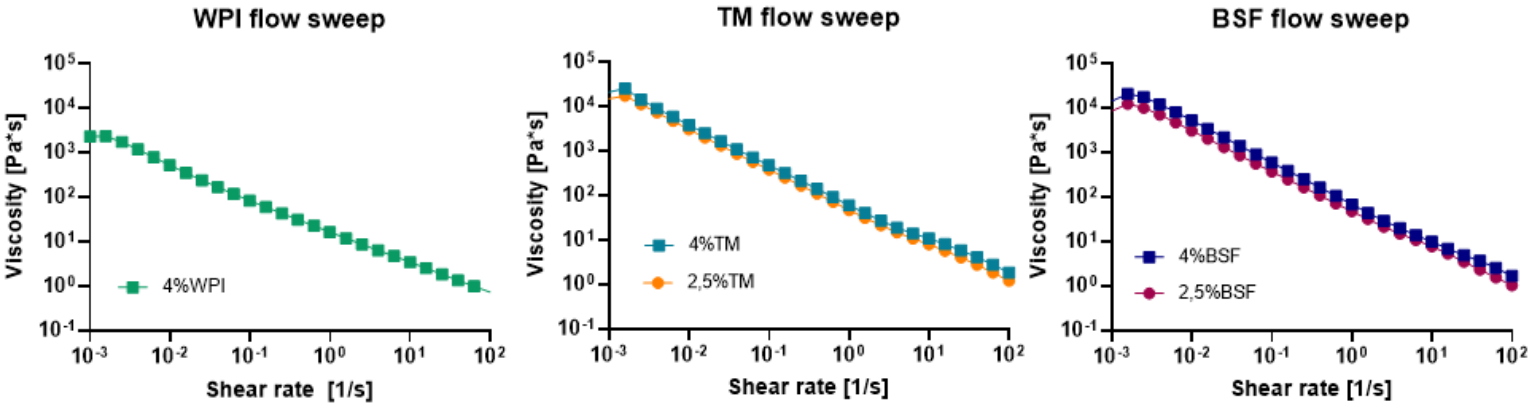

Figure 3 Flow sweeps of WPI, TM and BSF-stabilized emulsions.

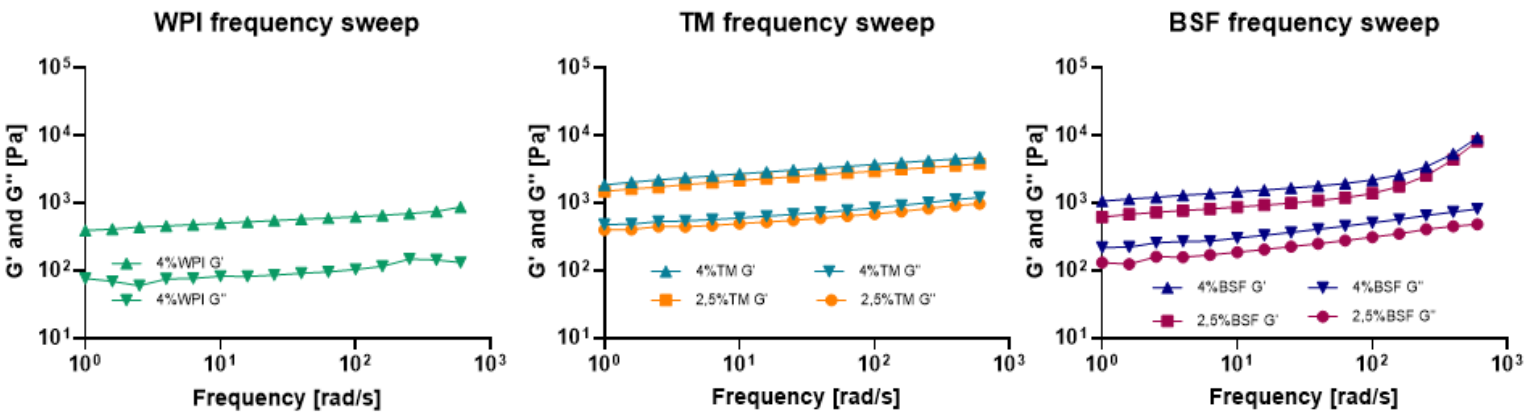

Figure 4 Frequency sweeps of WPI, TM and BSF-stabilized emulsions

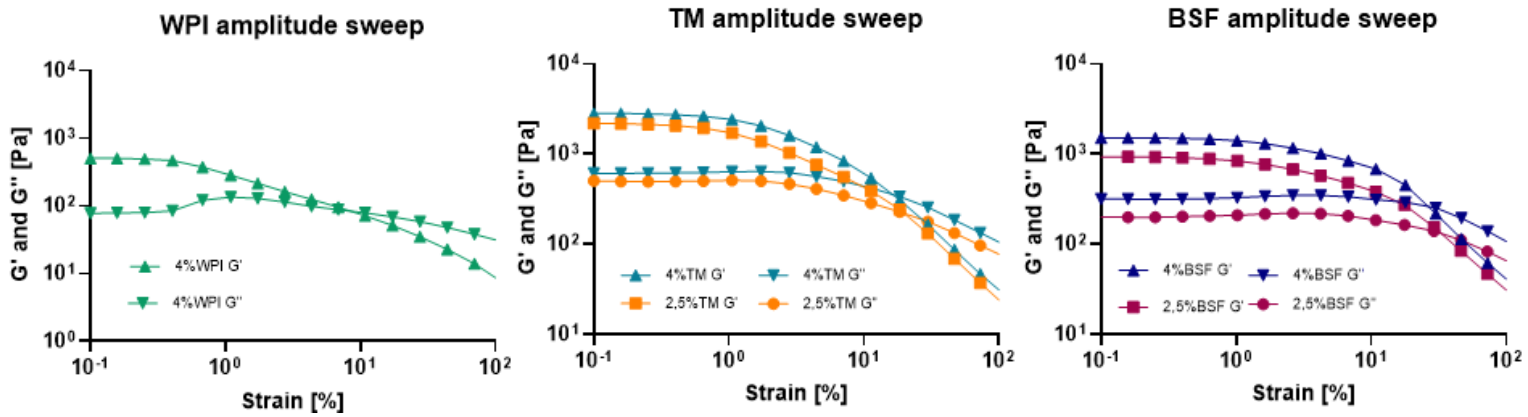

Figure 5 Amplitude sweeps of WPI, TM and BSF-stabilized emulsions.

3.4 3D printing

Finally, the potential of 4% WPI- and insect protein-stabilized HIPEs for 3D printing was evaluated. Of the HIPEs prepared, only those stabilized with 2.5% TMPC were unsuitable as ink under the tested printing conditions due to their overly liquid consistency (Fig. 6). This behavior may be partly attributed to particle size analysis, which showed that the emulsion stabilized with 2.5% TMPC exhibited a larger average droplet diameter. A coarser emulsion microstructure tends to promote droplet coalescence and phase separation, ultimately compromising the structural integrity of the system and negatively affecting its printability. Figure 7 shows the progression of the printed shapes

from immediately after printing (day 0) to 7 days of storage under room conditions. On day 0, the 4% WPI sample displayed slight spreading and lower shape definition compared to the good structural integrity observed in the other samples. The emulsions stabilized with 4% TM, 2.5% BSF, and 4% BSF maintained their ring-like geometries with minimal deformation immediately after printing. Over time, noticeable differences in shape stability emerged among the samples. The HIPE stabilized with WPI developed surface cracks by day 7, the 4% TM sample was completely melted beyond day 0 despite its initially high viscosity. The 2.5% BSF-stabilized HIPE showed clear signs of phase separation and oil leakage by day 7, while the 4% BSF sample appeared more porous but better retained its overall shape. However, both BSF-stabilized samples were not available for evaluation after day 7.

Figure 6 not-printable 2,5%TM stabilized HIPE.

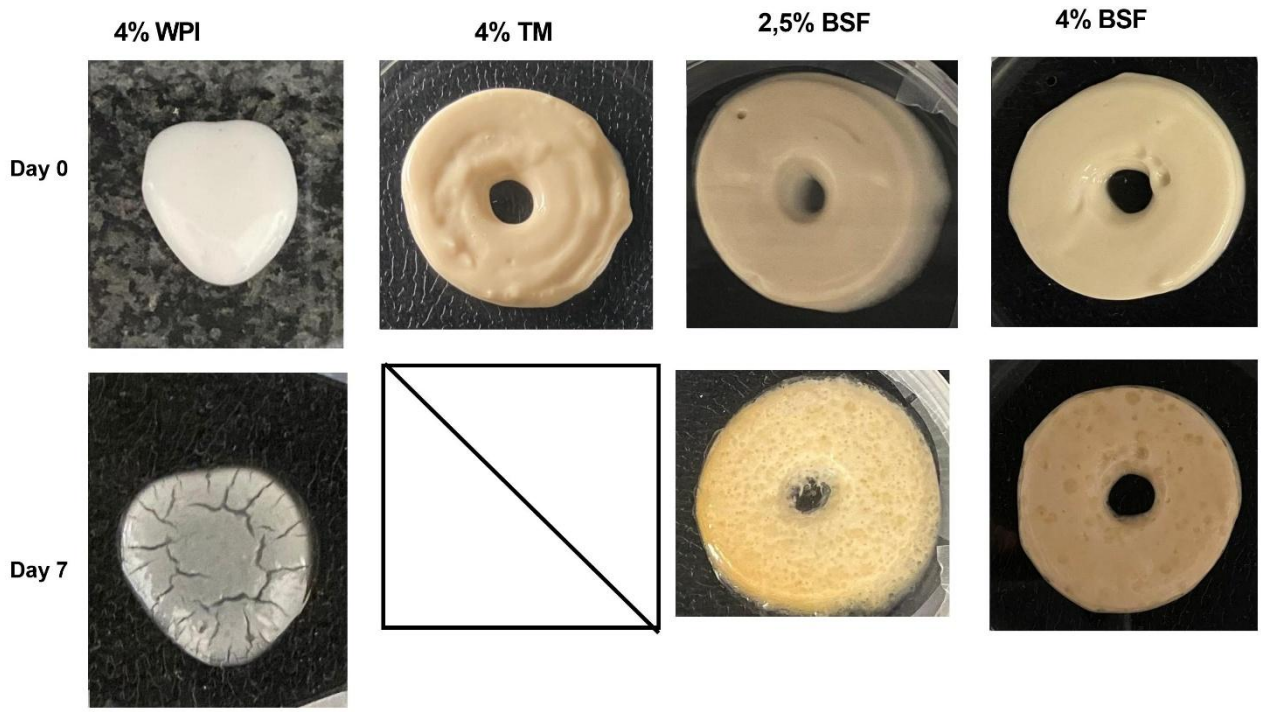

Figure 7 3D printed HIPEs at day 0 and day 7 at room temperature.

4 Conclusions

This study demonstrates that proteins derived from TM and BSF can effectively stabilize sunflower oil HIPEs, maintaining emulsion stability for 7 days. Although HIPEs stabilized with WPI remained stable for up to 22 days, insect protein-based emulsions exhibited superior rheological characteristics, including higher viscosity and consistently greater storage and loss moduli. These properties are advantageous for the development of fat analogues with desirable mechanical behavior. 3D printing trials further revealed that emulsions stabilized with insect proteins displayed improved shape fidelity immediately after printing compared to those stabilized with WPI. However, their structural integrity deteriorated after approximately one week. These findings highlight the promising functionality of insect-derived proteins in HIPE systems and their potential as sustainable fat analogue ingredients. Future work should focus on enhancing the long-term stability of these systems through formulation optimization and advanced processing techniques.

5 References

Ballon, A., Sessa, S., Cito, S., de Lamo-Castellví, S., Güell, C., & Ferrando, M. (2025). High internal phase emulsions stabilized by insect proteins: A path to 3D printable fat analogues. *Food Hydrocolloids, 166*, 111330. https://doi.org/10.1016/j.foodhyd.2025.111330

Bußler, S., Rumpold, B. A., Jander, E., Rawel, H. M., & Schlüter, O. K. (2016). Recovery and techno-functionality of flours and proteins from two edible insect species: Meal worm (Tenebrio molitor) and black soldier fly (Hermetia illucens) larvae. *Heliyon, 2*(12), e00218. https://doi.org/10.1016/j.heliyon.2016.e00218

Chen, Q.-H., Zheng, J., Xu, Y.-T., Yin, S.-W., Liu, F., & Tang, C.-H. (2018). Surface modification improves fabrication of pickering high internal phase emulsions stabilized by cellulose nanocrystals. *Food Hydrocolloids, 75*, 125–133. https://doi.org/10.1016/j.foodhyd.2017.10.019

Du, J., Dai, H., Wang, H., Yu, Y., Zhu, H., Fu, Y., Ma, L., Peng, L., Li, L., Wang, Q., & Zhang, Y. (2021). Preparation of high thermal stability gelatin emulsion and its application in 3D printing. *Food Hydrocolloids, 113*, 106536. https://doi.org/10.1016/j.foodhyd.2020.106536

Foegeding, E. A., & Davis, J. P. (2011). Food protein functionality: A comprehensive approach. *Food Hydrocolloids, 25*(8), 1853–1864. https://doi.org/10.1016/j.foodhyd.2011.05.008

Fuhrmann, P. L., Breunig, S., Sala, G., Windhab, E. J., & Fischer, P. (2022). Rheological behaviour of attractive emulsions differing in droplet-droplet interaction strength. *Journal of Colloid and Interface Science, 617*, 347–357. https://doi.org/10.1016/j.jcis.2022.04.022

Galvão, A. M. M. T., Vélez-Erazo, E. M., Bovi Karatay, G. G., de Figueiredo Furtado, G., Vidotto, D. C., Tavares, G. M., & Hubinger, M. D. (2022). High internal phase emulsions stabilized by the lentil protein isolate (Lens culinaris). *Colloids and Surfaces A: Physicochemical and Engineering Aspects, 653*, Article 129993. https://doi.org/10.1016/j.colsurfa.2022.129993

Gao, H., Ma, L., Cheng, C., Liu, J., Liang, R., Zou, L., Liu, W., & McClements, D. J. (2021). Review of recent advances in the preparation, properties, and applications of high internal phase emulsions. *Trends in Food Science & Technology, 112*, 36–49. https://doi.org/10.1016/j.tifs.2021.03.041

Gkinali, A.-A., Matsakidou, A., & Paraskevopoulou, A. (2022). Characterization of *Tenebrio molitor* larvae protein preparations obtained by different extraction approaches. *Foods, 11*(23), 3852. https://doi.org/10.3390/foods11233852

Gkinali, A.-A., Matsakidou, A., & Paraskevopoulou, A. (2023). Assessing the emulsifying properties of *Tenebrio molitor* larvae protein preparations: Impact of storage, thermal, and

freeze-thaw treatments on o/w emulsion stability. *International Journal of Biological Macromolecules, 250*, 126165. https://doi.org/10.1016/j.ijbiomac.2023.126165

Gould, J., & Wolf, B. (2018). Interfacial and emulsifying properties of mealworm protein at the oil/water interface. *Food Hydrocolloids, 77*, 57–65. https://doi.org/10.1016/j.foodhyd.2017.09.018

Hinderink, E. B. A., Schröder, A., Sagis, L. M. C., Schroën, K. G. P. H., & Berton-Carabin, C. C. (2021). Physical and oxidative stability of food emulsions prepared with pea protein fractions. *LWT – Food Science and Technology, 146*, Article 111424. https://doi.org/10.1016/j.lwt.2021.111424

Hu, X., & McClements, D. J. (2022). Construction of plant-based adipose tissue using high internal phase emulsions and emulsion gels. *Innovative Food Science & Emerging Technologies, 78*, 103016. https://doi.org/10.1016/j.ifset.2022.103016

Huang, D., Wu, Y., Li, W., Zhu, X., Liu, J., Jiang, Y., ... & Yu, Y. (2022). Advanced insight into the O/W emulsions stabilising capacity of water-soluble protein from *Tenebrio molitor*. *International Journal of Food Science and Technology, 57*(10), 6286–6297. https://doi.org/10.1111/ijfs.15746

Huang, X., Yan, C., Xu, Y., Ling, M., He, C., & Zhou, Z. (2023). High internal phase emulsions stabilized by alkaline-extracted walnut protein isolates and their application in food 3D printing. *Food Research International, 169*, 112858. https://doi.org/10.1016/j.foodres.2023.112858

Huang, X.-N., Zhou, F.-Z., Yang, T., Yin, S.-W., Tang, C.-H., & Yang, X.-Q. (2019). Fabrication and characterization of Pickering high internal phase emulsions (HIPEs) stabilized by chitosan-caseinophosphopeptides nanocomplexes as oral delivery vehicles. *Food Hydrocolloids, 93*, 34–45. https://doi.org/10.1016/j.foodhyd.2019.02.005

Huyst, A. M. R., Van der Meeren, P., Housmans, J. A. J., Monge-Morera, M., Rousseau, F., Schymkowitz, J., & Delcour, J. A. (2023). Improved coalescence and creaming stability of structured oil-in-water emulsions and emulsion gels containing ovalbumin amyloid-like fibrils produced by heat and enzymatic treatments. *Food Hydrocolloids, 145*, 109142. https://doi.org/10.1016/j.foodhyd.2023.109142

Jiang, H., Wang, X., Han, L., Tang, C., He, J., & Min, D. (2023). Intestine-targeted high internal phase Pickering emulsion formulated using silkworm pupa protein via ultrasonic treatment. *International Journal of Biological Macromolecules, 246*, 125620. https://doi.org/10.1016/j.ijbiomac.2023.125620

Liu, G., Li, W., Qin, X., & Zhong, Q. (2020). Pickering emulsions stabilized by amphiphilic anisotropic nanofibrils of glycated whey proteins. *Food Hydrocolloids, 101*, 105503. https://doi.org/10.1016/j.foodhyd.2019.105503

Shi, A., Feng, X., Wang, Q., & Adhikari, B. (2020). Pickering and high internal phase Pickering emulsions stabilized by protein-based particles: A review of synthesis, application and prospective. *Food Hydrocolloids, 109*, 106117. https://doi.org/10.1016/j.foodhyd.2020.106117

Sun, C., Wang, S., Wang, S., Wang, P., Zhang, G., Liu, H., Zhu, D. (2024). Characterization of high-internal-phase emulsions based on soy protein isolate with varying concentrations of soy hull polysaccharide and their capabilities for probiotic delivery: In vivo and in vitro release and thermal stability. *Food Research International, 186*, 114371. https://doi.org/10.1016/j.foodres.2024.114371

Van Huis, A., Van Itterbeeck, J., Klunder, H., Mertens, E., Halloran, A., Muir, G., & Vantomme, P. (2013). *Edible insects: Future prospects for food and feed security*. FAO Forestry Paper 171. Rome: Food and Agriculture Organization of the United Nations.

Wang, J., Ballon, A., Schröen, K., de Lamo-Castellví, S., Ferrando, M., & Güell, C. (2021). Polyphenol loaded W1/O/W2 emulsions stabilized with lesser mealworm (*Alphitobius diaperinus*) protein concentrate produced by membrane emulsification: Stability under simulated storage, process, and digestion conditions. *Foods, 10*(12), 2997. https://doi.org/10.3390/foods10122997

Wang, J., Jousse, M., Jayakumar, J., Fernández-Arteaga, A., de Lamo-Castellví, S., Ferrando, M., & Güell, C. (2021). Black soldier fly (*Hermetia illucens*) protein concentrates as a sustainable source to stabilize O/W emulsions produced by a low-energy high-throughput emulsification. *Foods*. https://doi.org/10.3390/foods10122997

Wang, Y., Yang, H., Tian, Y., Li, T., Wang, Y., Zhang, X., Huang, J., Xia, B., Wang, S., & Dong, W. (2025). Zein-cyclodextrin complex used to prepare high internal phase pickering emulsions with various oil phases. *Colloids and Surfaces A: Physicochemical and Engineering Aspects, 704*, 135506. https://doi.org/10.1016/j.colsurfa.2024.135506

Yan, G., Li, Y., Wang, S., Li, Y., Zhang, L., Yan, J., & Sun, Y. (2024). Oil–water interfacial behaviour of different caseins and stability of emulsions: Effect of micelle content and caseins concentrations. *Food Chemistry: X, 23*, 101784. https://doi.org/10.1016/j.fochx.2024.101784

Zhang, M., Fan, L., Liu, Y., Huang, S., & Li, J. (2022). Effects of proteins on emulsion stability: The role of proteins at the oil–water interface. *Food Chemistry, 397*, 133726. https://doi.org/10.1016/j.foodchem.2022.133726